Predicting the operability limit of the HyShot II scramjet using LES

J. Larsson, I. Bermejo-Moreno, J. Bodart, Ronan Vicquelin

Predicting the operability limit of the HyShot II scramjet using LES

By J. Larsson, I. Bermejo-Moreno, J. Bodart AND R. Vicquelin

1. Motivation and objectives

The present work is part of a broad effort toward predictive simulations of complex multi-physics flows at high Reynolds numbers. The main objective of the Stanford PSAAP Center (Predictive Science Academic Alliance Program) is to predict the reacting flow in the HyShot II scramjet experiment carried out in the High Enthalphy shock tunnel at Göttingen (HEG) facility of the German Aerospace Agency DLR (cf. Gardner *et al.* 2004; Laurence *et al.* 2012). Specifically, the objective is to predict the best-estimate of the flow, to estimate the uncertainties from a range of sources in this prediction and, finally, to quantify the margin to engine unstart.

Scramjet combustors are designed to use the heat added from combustion to cause an increase in pressure, which, when expanded in a nozzle, causes thrust. At nominal conditions, the HyShot II is designed to have essentially attached flow throughout the combustor, with a smooth (not counting the many oblique shock waves) rise in pressure throughout. If too much fuel is injected, leading to excessive heat addition, the flow may become choked; this would initiate an unsteady "unstart" process, eventually resulting in subsonic flow throughout the combustor and complete loss of thrust. This failure mode is abrupt and catastrophic. The objective of the present work is to characterize the flow in the regime separating nominal operating conditions from catastrophic unstart. This is done using a combination of large eddy simulations (LES) and experimental data from a recent study by Laurence *et al.* (2012). Preliminary results of the LES study were reported in Larsson *et al.* (2011).

The fact that LES directly resolves the largest turbulent structures implies that it, generally speaking, leads to more accurate predictions of mixing than RANS is capable of. Mixing is a key phenomenon in supersonic combustion; in many cases it is the rate-controlling process. LES can therefore be expected to yield more accurate and trustworthy predictions than RANS (cf. Fulton *et al.* 2012, for a direct comparison for a relevant flow). A nice summary of the current state-of-the-art and different approaches in LES of scramjet flows is provided in Fureby (2012).

The complexity of the flow (turbulence, shocks, mixing, combustion) implies that a careful multi-stage validation plan is needed. Moreover, the available quantitative experimental data for the HyShot case is limited to measurements of pressure (mean and rms) and heat transfer (considered uncertain) along two lines in the combustor. Therefore, validation on the HyShot problem alone is not sufficient. The first step in the validation is to compute a supersonic flat plate boundary layer as a basic check on the LES method and, specifically, the modeling of the friction and heat transfer at the wall; this was reported in Larsson *et al.* (2011), where a full description of the wall-model was also provided. The next validation step is the duct flow with shock/boundary layer interactions studied experimentally by Helmer *et al.* (2012). This problem validates the capability of the wall-modeled LES to capture stress-induced secondary corner flows and, most importantly,

shock/boundary layer interaction; results from this validation exercise are described in Bermejo-Moreno *et al.* (2011). The third validation problem is the experiments of the so-called "CESCo" model combustor by Gamba *et al.* (2011). These experiments are ongoing, and will include both toluene PLIF (planar laser-induced fluorescence) thermometry measurements of the cold flow (Miller *et al.* 2011) and several quantitative measurements of the reacting flow problem.

2. Methodology

The filtered compressible Navier-Stokes equations are solved for the conserved variables. For reacting flow, the total energy is defined as the sum of sensible, kinetic and chemical energy. The residual subgrid stress is modeled using an eddy-viscosity hypothesis together with the model by Vreman (2004). The subgrid heat flux and species transport are modeled using gradient hypotheses with fixed turbulent Prandtl and Schmidt numbers, both taken as 0.5. The equations are implemented in the unstructured code *CharlesX*, which uses a solution-adaptive approach mathematically analyzed in a set of papers (Larsson & Gustafsson 2008; Larsson 2010) in which a non-dissipative scheme with low aliasing error is used away from shock waves while an unstructured essentially non-oscillatory (ENO) second-order accurate shock-capturing scheme is applied near discontinuities. At each time step, the shock-capturing scheme is applied if the negative rate of dilatation $-\partial_j u_j > \max\left(\sqrt{\omega_j\omega_j}, 0.1\,c/h\right)$, where ω_j is the vorticity and c/h is the speed-of-sound divided by the cell size. The shock-capturing scheme is additionally applied if two adjacent cells differ by more than 500 K in temperature, by more than 0.4 in the mixture fraction or by more than 0.2 in the mass fraction of H_2O.

2.1. *Wall-model*

The wall-model and the reasons why it is necessary in the HyShot combustor were laid out in last year's report (Larsson *et al.* 2011), thus only a brief description is given here. First, the friction Reynolds number of the boundary layers in the HyShot combustor ranges from 1500 to 4000. Together with the large dimensions of the combustor, this implies that at least 100 billion grid points would be needed in order to perform a traditional, wall-resolved, LES. Secondly, one can estimate (Larsson *et al.* 2011) that the pressure rise in the HyShot combustor is due in roughly equal parts to heat addition from combustion, wall friction and wall heat losses; the former two increases the pressure while the latter decreases it. Therefore, accurate modeling/capturing of the near wall processes is just as crucial as accurate modeling of the combustion-generated heat release.

To this end, the equilibrium wall-model and the associated technique for connecting it with the LES developed by Kawai & Larsson (2012) is used here. Briefly, the wall-model consists of two ODEs in the wall-normal direction for streamwise momentum and total energy, respectively, where convection and pressure-gradient effects have been neglected. Moreover, the scalar mixture composition is assumed constant normal to the wall. More details along with validation cases can be found in the references cited here.

2.2. *Combustion model*

The Stanford H_2/O_2 mechanism (9 species, 20 reactions) by Hong *et al.* (2011) is used to model the chemical reactions together with a steady flamelet/progress-variable method. Flamelet-based models with a presumed PDF have been rather widely used in the area of subsonic combustion, but have rarely been applied to supersonic combustion. For example, the LES study of the HyShot II scramjet by Fureby *et al.* (2011) solved transport

equations for the species at the macro-level using a partially stirred reactor model to close the chemical source terms. Similarly, the LES of Edwards *et al.* (2012) solved macro-level transport equations, but without any special closure for the source term. The chief difficulty in applying a flamelet model to supersonic combustion is the hydrodynamically induced variations in pressure and enthalpy (e.g., shock waves, wall cooling, etc). Since the flamelets are solved a priori with the results tabulated for later use in the LES, it is clear that there is a lack of feedback from the LES solver to the flamelet solver. In the present work, the flamelets are solved at a single fixed reference pressure of 1.5 bar, and at fixed temperatures at the fuel and oxidizer boundaries. In the LES, the pure fuel expands essentially isentropically, and reaches 210 K at the flamelet reference pressure. There is little variability from this isentropic expansion, and thus the fuel temperature in the flamelet model is relatively certain (though it should, of course, vary with pressure). The air, on the other hand, is compressed by shocks and strongly cooled in the vicinity of the walls, and thus a wide range of air temperatures co-exist in the combustor. A representative value of 1500 K is used in the flamelet calculations, but it should be noted that the use of a constant air temperature introduces errors in the model.

While the pressure and boundary temperatures in the flamelet model are fixed, hydrodynamic effects will produce large variations in the actual LES fields. In the present work we follow the approach of Pecnik *et al.* (2012), where the species mass fractions are assumed to be independent of the pressure and the flamelet boundary temperatures, whereas the source term of the reaction progress variable is assumed to scale with the square of pressure (since the majority of the reactions are bimolecular). The FlameMaster code is used to compute the steady diffusion flamelets in a counterflow setting.

The effect of turbulence on the small-scale chemistry is modeled by a presumed β probability density function (PDF) for the mixture fraction Z. For the reaction progress variable C, a δ distribution is assumed. At the macro-scale (LES) level, additional transport equations are solved for the filtered mixture fraction $\widetilde{Z}$, the subfilter variance $\widetilde{Z''Z''}$ and the filtered progress variable $\widetilde{C}$.

We point out that the present work is focused on predicting the gross features of the scramjet, specifically the pressure-rise in the combustor, with no emphasis placed on the prediction of minor species at all. The flamelet/progress-variable turbulent combustion model used here reflects these objectives. Specifically, we note that the assumption of a chemical composition that does not depend on pressure or fuel/oxidizer temperatures is somewhat heroic.

3. Results

Figure 1 shows a RANS result for the reacting flow in the HyShot II scramjet. The shock-trap and the leading edge of the lower wall are visible at the far left of the figure, as is the fuel injector about 60 mm farther downstream. The domain for the LES is chosen to start between these two locations, at the location of the vertical line in Fig. 1. There are several reasons for choosing this point as the LES inlet. To minimize the cost, the inlet should be as close to the injector as possible, but sufficiently far upstream that the inflow turbulence becomes developed and the injector bow shock is captured properly. In addition, the inlet should not be placed at a point where the oblique shock-train is near the wall, where a shock/boundary layer interaction occurs. Having chosen the inlet location, the inflow profiles are taken from RANS and used in the synthetic turbulent inflow generation.

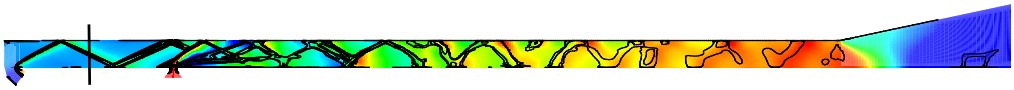

FIGURE 1. Slice through the injector from a RANS simulation at the nominal operating condition. Contours of pressure showing the gradual increase caused by combustion, overlaid with contour lines of large negative dilation showing the strongest shocks. The vertical line before the injector shows the location of the inflow for the LES.

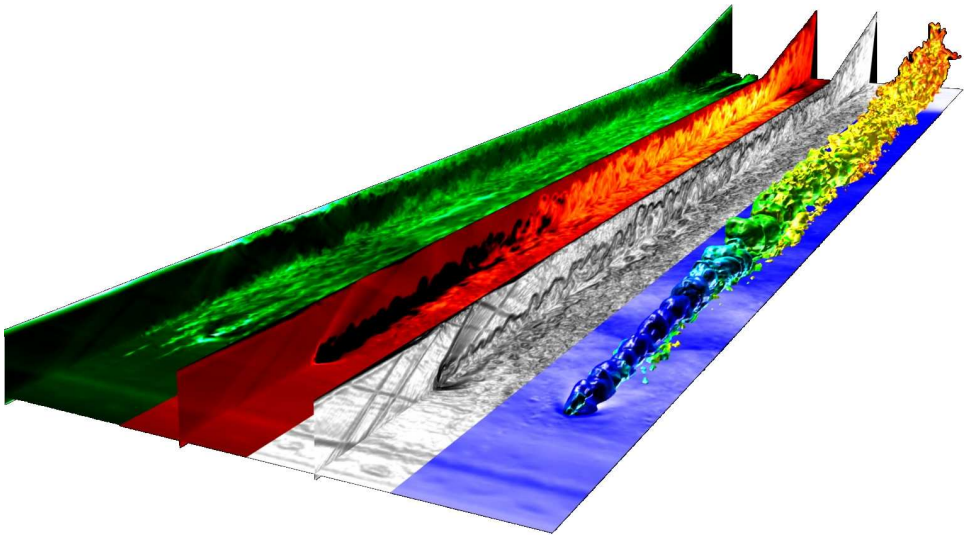

FIGURE 2. Instantaneous snapshot from LES of the HyShot II combustor. The computational domain (one injector) is replicated four times in the spanwise direction. From the left, the slices show contours of streamwise velocity u_1, temperature T, simulated Schlieren $|\nabla\rho|$, and pressure p. In addition, the right-most section shows an isosurface at the stoichiometric mixture fraction, colored by the OH concentration.

The full HyShot II combustor is 75 mm wide with four fuel injectors spaced equidistantly. Only a single injector (i.e., 1/4 of the full combustor width) is computed with LES, assuming periodic boundary conditions in the spanwise direction. This approximation is expected to be reasonable, since the RANS study by Pecnik *et al.* (2012) showed relatively minor effects of the combustor side walls. The walls are assumed isothermal at 300 K due to the short duration of the shock-tube experiments.

An instantaneous snapshot from the LES is shown in Fig. 2. The multiple incoming oblique shock waves are visible in the Schlieren image, as is the strong bow shock around the fuel injector. The fuel jet is initially relatively unperturbed, but breaks down into full turbulence farther downstream. The velocity contours show the thin incoming boundary layers and how these grow farther downstream. Finally, the temperature contour shows how the heat release leads to increased temperatures downstream, up to about 2500 K before the nozzle.

The grids are mainly structured, with O-grids in and around the fuel injector. Three different grids are used to estimate the degree of grid sensitivity in the results, with total

cell-counts of $100 \cdot 10^6$ (fine), $43 \cdot 10^6$ (medium) and $14 \cdot 10^6$ (coarse). The spanwise grid spacing throughout the domain, and the streamwise grid spacing in the region around the fuel injector, is 0.075, 0.10 and 0.15 mm for the three grids, respectively. The streamwise grid spacing is stretched by a factor of two towards the inlet, and by a factor of three towards the region where the combustion occurs. The wall-normal grid spacing is equal to the spanwise one in the core of the combustor, and stretched by a factor 0.3 towards the walls.

The boundary layers are approximately 1 mm thick throughout most of the domain (slightly thinner near the inlet, slightly thicker in the combustor region); thus the grid resolution is somewhat coarse in the boundary layers compared to the criteria given by Kawai & Larsson (2012). Note that the wall-model is not applied in the injector itself, since the flow there is laminar due to the strong contraction.

The simulations are run for about 1-2 ms, which is a bit shorter than, but comparable to, the actual test time in the shock tube. About $250 \cdot 10^3$, $120 \cdot 10^3$ and $20 \cdot 10^3$ core-hours are needed for the three grids, respectively. These numbers are valid for started flow at nominal equivalence ratios (far from the unstart bound); simulations closer to the operability limit must be run for much longer, as will be discussed below.

3.1. *Validation at started conditions*

The first experimental campaign in the HEG shock-tube at DLR in Germany (cf. Gardner *et al.* 2004) considered two different operating conditions, replicating the flight conditions at altitudes of 27 and 33 km, respectively. All simulations performed at the Stanford PSAAP Center have focused on the 27 km case.

A total of 9 experimental shots with reacting flow near the nominal operating condition are available from the campaign by Gardner *et al.* (2004); these have nominal equivalence ratios from 0.27 to 0.35 due to shot-to-shot variations. The equivalence ratio (ER) is defined as the ratio of the actual fuel mass flux compared to the fuel mass flux which would produce globally stoichiometric burning. The shot with the highest ER (shot #810) is chosen for the validation study, since this can be expected to be the most challenging. To estimate the uncertainty in the measurements, the variation in the measured values for the 3 shots with the highest ERs (having nominal ERs of 0.33, 0.34, 0.35) is used as a rough estimate of the shot-to-shot variability or measurement uncertainty; this min/max range is shown with errorbars in the figures. The total pressure and temperature of the hydrogen fuel for shot #810 are 5.73 bar and 300 K, respectively.

The quantitative experimental data available are measurements of pressure and heat flux along lines on the lower and upper walls in the combustor for the 9 experimental shots. The comparison between this data and the LES results is shown in Figs. 3 and 4.

We first note that the LES results for the mean pressure on the three grids are relatively close to each other, indicating that the results are close to grid-converged for this quantity. The experimental results suggest large variations between subsequent pressure taps; the LES, on all three grids, has much lower variation in the mean pressure. The reason for this discrepancy is not clear: the obvious explanation would be that the (numerically captured) shocks in the LES are smeared, but if this were the case there should be a larger difference between the results from the three grids.

The computed mean pressure profiles fall along the upper bound of the experimental data. The rms pressure fluctuations also fall within with experimental bounds, although consistently overpredicting the measured values for the same experimental shot. The computed wall heat flux agrees quite well with the measurements, though less well for the upper wall.

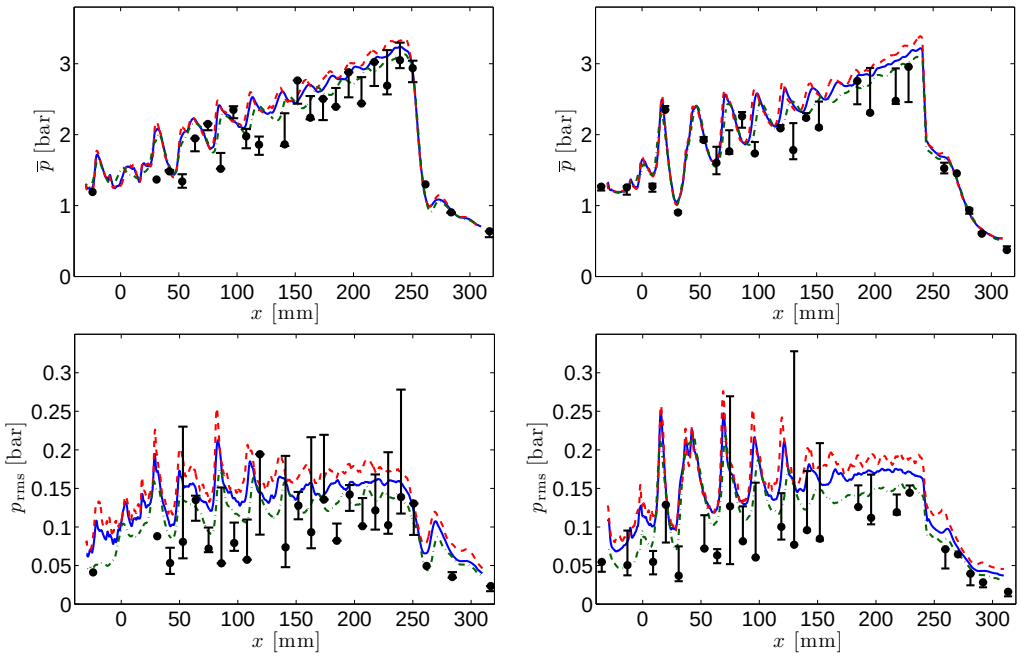

FIGURE 3. Wall pressure along lines halfway between the injectors in HyShot II from LES (lines) compared with experiment by Gardner *et al.* (2004) for shot #810 with ER=0.35. Experimental value for that shot (circles) and the min/max among 3 shots with ER=0.33–0.35 (errorbars) as an estimate of shot-to-shot variation. LES on fine mesh (100M cells, dashed), medium mesh (43M cells, solid) and coarse mesh (14M cells, dash-dotted). Top row: Average pressure. Bottom row: Rms pressure fluctuation. Left column: Lower wall. Right column: Upper wall.

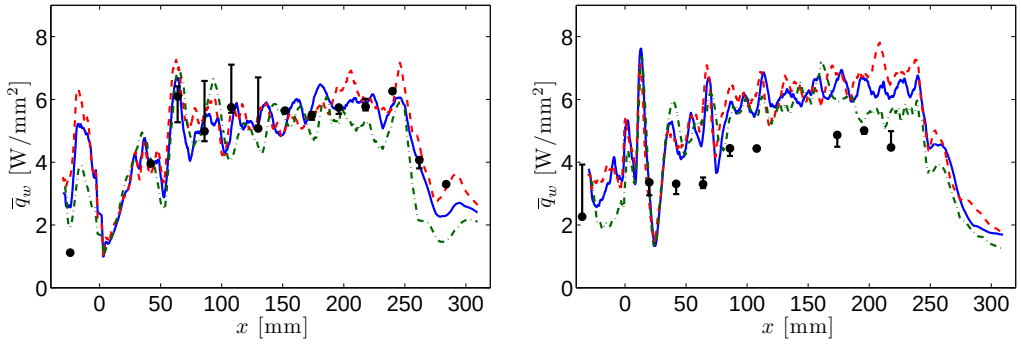

FIGURE 4. Mean wall heat flux along lines through the injector in HyShot II from LES (lines) compared with experiment by Gardner *et al.* (2004) for shot #810 with ER=0.35. Experimental value for that shot (circles) and the min/max among 3 shots with ER=0.33–0.35 (errorbars) as an estimate of shot-to-shot variation. LES on fine mesh (100M cells, dashed), medium mesh (43M cells, solid) and coarse mesh (14M cells, dash-dotted). Left: Lower wall. Right: Upper wall.

While the mean pressure is essentially grid-converged, the rms of the pressure fluctuations increases as the grid is refined. This is expected in LES, as more turbulent structures are resolved. We also note that the wall heat flux shows a larger difference between the coarse and medium grids than the mean pressure did. This is, to some degree,

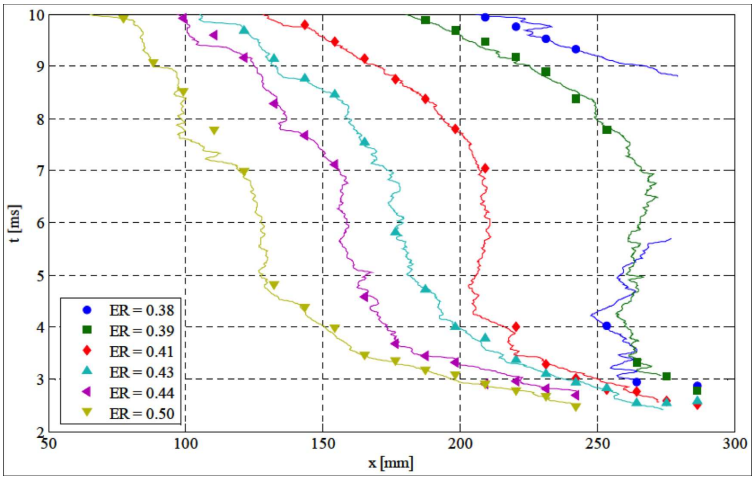

FIGURE 5. Instantaneous location of the leading (and strongest) shock in the shock-train from the experiments of Laurence *et al.* (2012). The shock location is deduced in two ways, with both shown in the figure: using Schlieren images (lines) and using pressure transducers (symbols). Figure adapted from Laurence *et al.* (2012); note that the x coordinate should be decreased by 57.5 mm to correspond to the present simulations.

consistent with the higher level of turbulence implied by the pressure rms results. Finally, the difference between the LES and the experiments is larger on the upper wall than on the lower wall, at least for the pressure rms and the mean wall heat flux. The fuel jet in HyShot does not penetrate very far, and thus the upper boundary layer is relatively undisturbed. On the lower wall, on the other hand, the boundary layer is completely affected by the fuel injection. One possible explanation for this discrepancy is that the wall-model, which assumes equilibrium, is simply inaccurate on the lower wall. While plausible, the length of the combustor is such that the boundary layer should return to something close to equilibrium, but the discrepancy persists; thus this explanation may not be the full story. Another possible explanation is the combustion model: if it predicts too much burning near the wall, then the wall heat flux would certainly be overpredicted. A deeper analysis of these results is underway.

3.2. *Investigating the operability limit*

The HyShot II scramjet is designed to have a "smooth" (not counting the many oblique shocks) rise in pressure; the pressure profiles in Fig. 3 are typical of nominal or safe operation. Excessive heat addition (or friction) may cause any supersonic internal flow to choke and subsequently unstart. The signature of choking is the appearance of a stronger shock, one example of which is the dash-dotted line in Fig. 7. A choked flow produces no thrust and is thus clearly undesirable. The main objective of the present study is to investigate the behavior of the flow around the operability limit, between safe and undesirable operation.

Partly spurred by the attempts to investigate the operability limit using LES in this study, DLR decided to launch a new experimental campaign in 2012 specifically targeting operating conditions around the operability limit. Preliminary results from this experimental study were reported in Laurence *et al.* (2012), from which Fig. 5 was extracted.

Flow visualizations show the formation of a shock-train at high ERs. The figure shows the location of this leading shock as a function of time for different experimental shots.

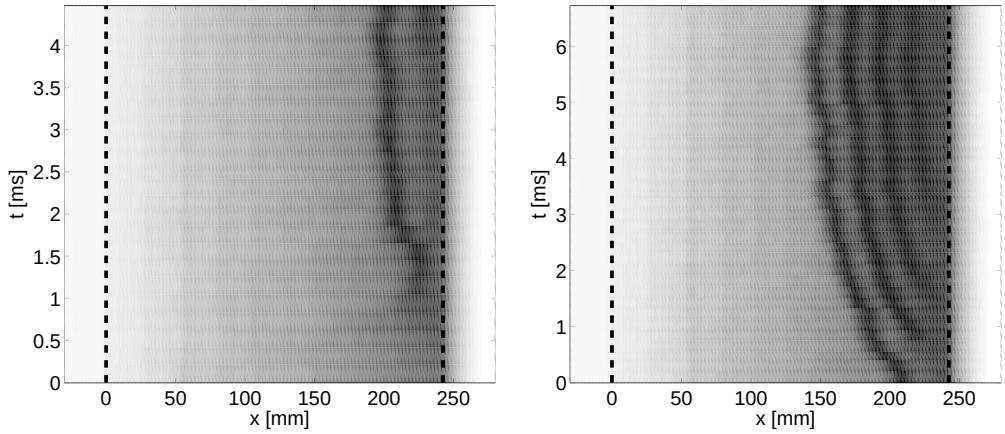

FIGURE 6. Pressure averaged across the combustor cross-section from the medium mesh, plotted versus streamwise location and time in grayscale from low (white) to high (black) values. The thick dashed lines denote the locations of the injector and the beginning of the nozzle, respectively. Left: ER=0.40. Right: ER=0.41.

Note that the steady part of the test time is from $t \approx 4.5$ ms to $t \approx 7$ ms. During this time, the shock position is almost steady. Whether exactly steady or simply drifting upstream very slowly is impossible to tell due to the short test time.

Essentially similar figures from the LES results are shown in Fig. 6. The highest pressures form a "ridge" in the figures; the location of the front part of this ridge corresponds to the shock locations defined for the experiment in Fig. 5.

Before comparing the LES and the experiment, we first note that the origin of the x coordinate differs by 57.5 mm in the two cases. Secondly, and much more importantly, we note that the LES computations were performed before the experiment was conducted. Specifically, the LES computations use the nominal shock-tube conditions from the Gardner *et al.* (2004) campaign. However, as explained in Laurence *et al.* (2012), the shock-tube conditions in the most recent experimental study differ slightly, by about 5% in the shock-tube stagnation pressure. This discrepancy is partially accounted for here by scaling the experimental pressure data by the stagnation pressures.

The experimental result at ER=0.41 suggests a quasi-steady shock location at $x \approx 150$ mm (in LES coordinates). The LES at that ER does not show unambiguously that the shock has stopped moving, only that the speed of this shock decreases as it moves upstream. These simulations require a lot of time steps and are still running. As of this writing, the shock is at $x \approx 140$ mm, which is rather close to the experimental value, especially considering the known differences in the shock-tube conditions.

The experimental pressure profiles averaged during the quasi-steady test time are compared with profiles averaged during the last 0.2 ms of the LES runs in Fig. 7. The first thing to notice is the collapse of the pressure profiles up to the leading shock in the shock-train among both the experimental shots and the simulation results. This is due to the low momentum flux ratio at these ERs, coupled with the fact that the combustion during the initial phase is insensitive to the amount of fuel injected. There is a qualitative agreement between the computed and experimental results at each ER, although the simulations consistently show higher pressure and a leading shock (for the two highest ERs) that is slightly more upstream.

It is impossible to interpret these results until the simulations have run for sufficiently

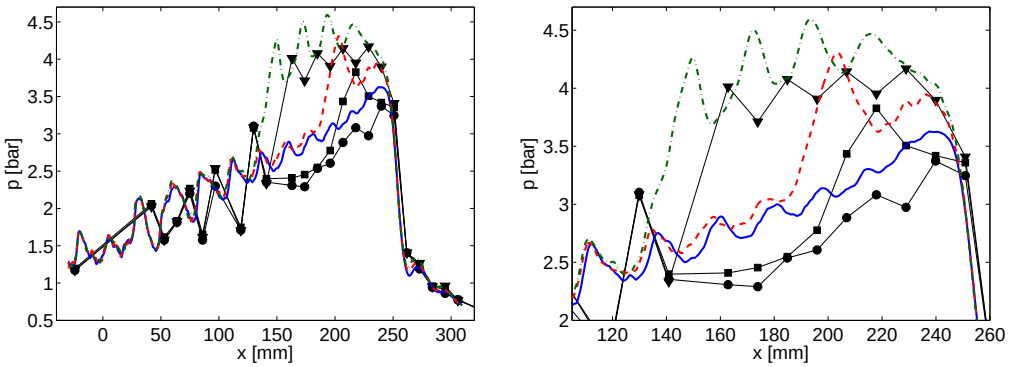

FIGURE 7. Mean wall pressure on the lower wall halfway between the injectors from LES (lines) and experiments by Laurence *et al.* (2012) (symbols). LES results at ER of 0.38 (solid), 0.40 (dashed) and 0.41 (dash-dotted); averaged over the last 0.2 ms in Fig. 6 of the still running calculations. Experimental results at ER of 0.38 (circles), 0.39 (squares) and 0.41 (triangles); averaged over the quasi-steady test time in Fig. 5. Full view (left) and zoomed (right).

long times to really unambiguously show whether or not a steady state is reached. If the simulations truly reach steady states, then comparison of those ER-dependent steady states with the experiment becomes meaningful. If the simulations never reach a steady state, then either the simulations are wrong in this very fundamental way or the short test time of the experiments limits their utility.

Having said this, what *can* be concluded at this stage is that both the experiment and the LES produce steady flow with essentially linear pressure rises with x at ER=0.38. Even more, they both show the appearance of a stronger shock-train near the end of the combustor at the next higher ER (0.39 in the experiment, 0.40 in the LES). Therefore, regardless of whether there exist steady state solutions at some range of intermediate ERs, there is excellent agreement between the LES and the experiment on the fact that the pressure profile is essentially linear and that the solution is steady for ER $\lesssim$ 0.38. This defines a regime of completely safe operation.

4. Summary and future work

This paper describes ongoing work toward predictive large eddy simulations (LES) of the reacting flow in the HyShot II scramjet combustor, specifically focused on the solutions near the limit of operability. The high Reynolds number makes traditional LES completely impractical, and thus a wall-model for the innermost portion of the boundary layers is needed. The combustion chemistry is parametrized through the flamelet/progress-variable approach, with a presumed PDF for the mixture fraction. The strength of this modeling approach is the direct resolution of the flame micro structure and the fact that turbulence-induced subgrid fluctuations of the mixture fraction are accounted for; the main weaknesses of this modeling approach (in its current form) are the inability to predict auto-ignition (in the steady flamelet framework) and the lack of feedback from flow-induced changes in pressure and enthalpy on the combustion chemistry. These issues are part of ongoing research; however, it must be noted that the main objective of the present study is to predict the pressure-rise in the combustor, rather than minor species concentrations. The predicted pressure-rise is within the experimental bounds, and shows reasonable grid-convergence.

With this verification/validation study in hand, the simulation methodology is then used to determine the unstart bound. This is done by keeping the shock tube conditions fixed while increasing the total pressure of the fuel stream in finite steps. The LES and the experiments both show steady state solutions with linear pressure profiles for ERs $\lesssim 0.38$, and the appearance of a stronger shock-train near the end of the combustor for ERs $\gtrsim 0.40$ and 0.39, respectively (note that no LES has been run at ER=0.39). For the purpose of defining an operability limit to be used in the mission of the Stanford PSAAP Center, this result is sufficient: one would not want to operate a scramjet with a strong shock-train near the end, and thus the limit of safe operation is between ERs of approximately 0.38 and 0.39.

Beyond this purpose, there is, of course, great interest in finding out whether there truly exist steady state solutions at some intermediate range of ERs above 0.38 but not so high that a true unstart process occurs. The only possible way to investigate this is to run the current LES calculations for much longer times.

Acknowledgments

This work is supported by the Department of Energy Predictive Science Academic Alliance Program (PSAAP; grant DE-FC52-08NA28614). The work on wall-modeling is supported by the Air Force Office of Scientific Research (grant FA9550-11-1-0111). Computing resources are partially provided through the American Recovery and Reinvestment Act of 2009, through the NSF-funded Certainty cluster. The work has benefitted from stimulating discussions with Mirko Gamba and Stuart Laurence, as well as insightful comments by Carlo Scalo.

REFERENCES

Bermejo-Moreno, I., Larsson, J., Campo, L., Bodart, J., Vicquelin, R., Helmer, D. & Eaton, J. 2011 Wall-modeled large eddy simulation of shock/turbulent boundary-layer interaction in a duct. In *Annu. Res. Briefs*, pp. 49–62. Center for Turbulence Research.

Edwards, J. R., Boles, J. A. & Baurle, R. A. 2012 Large-eddy/Reynolds-averaged Navier-Stokes simulation of a supersonic reacting wall jet. *Combust. Flame* **159**, 1127–1138.

Fulton, J., Edwards, J. R., Hassan, H. A., Rockwell, R., Goyne, C., McDaniel, J., Smith, C., Cutler, A., Johansen, C., Danehy, P. M. & Kouchi, T. 2012 Large-eddy/Reynolds-averaged Navier-Stokes simulations of a dual-mode scramjet combustor. AIAA Paper 2012-0115.

Fureby, C. 2012 LES for supersonic combustion. AIAA Paper 2012-5979.

Fureby, C., Chapuis, M., Fedina, E. & Karl, S. 2011 CFD analysis of the HyShot II scramjet combustor. *Proc. Comb. Inst.* **33**, 2399–2405.

Gamba, M., Miller, V. A., Mungal, M. G. & Hanson, R. K. 2011 Ignition and flame structure in a compact inlet/scramjet combustor model. AIAA Paper 2011-2366.

Gardner, A. D., Hannemann, K., Steelant, J. & Paull, A. 2004 Ground testing of the HyShot supersonic combustion flight experiment in HEG and comparison with flight data. AIAA Paper 2004-3345.

Helmer, D. B., Campo, L. M. & Eaton, J. K. 2012 Three-dimensional features of a Mach 2.1 shock/boundary layer interaction. *Exp. Fluids* (to appear).

Hong, Z., Davidson, D. F. & Hanson, R. K. 2011 An improved H2/O2 mechanism based on recent shock tube/laser absorption measurements. *Combust. Flame* **158**, 633–644.

Kawai, S. & Larsson, J. 2012 Wall-modeling in large eddy simulation: length scales, grid resolution and accuracy. *Phys. Fluids* **24**, 015104.

Larsson, J. 2010 Effect of shock-capturing errors on turbulence statistics. *AIAA J.* **48** (7), 1554–1557.

Larsson, J. & Gustafsson, B. 2008 Stability criteria for hybrid difference methods. *J. Comput. Phys.* **227**, 2886–2898.

Larsson, J., Vicquelin, R. & Bermejo-Moreno, I. 2011 Large eddy simulations of the HyShot II scramjet. In *Annu. Res. Briefs*, pp. 63–74. Center for Turbulence Research.

Laurence, S. J., Ozawa, H., Lieber, D., Schramm, J. M. & Hannemann, K. 2012 Investigation of unsteady/quasi-steady scramjet behavior using high-speed visualization techniques. AIAA Paper 2012-5913.

Miller, V. A., Gamba, M., Mungal, M. G. & Hanson, R. K. 2011 Toluene PLIF thermometry and imaging in supersonic flows. In *Annu. Res. Briefs*, pp. 273–284. Center for Turbulence Research.

Pecnik, R., Terrapon, V. E., Ham, F., Iaccarino, G. & Pitsch, H. 2012 Reynolds-averaged Navier-Stokes simulations of the HyShot II scramjet. *AIAA J.* **50** (8), 1717–1732.

Vreman, A. W. 2004 An eddy-viscosity subgrid-scale model for turbulent shear flow: Algebraic theory and applications. *Phys. Fluids* **16** (10), 3670–3681.